Supporting Information for

Optimized Loopable Translation as a Platform for the Synthesis of Repetitive Proteins

Sea On Lee[1], Qi Xie[1], Stephen D. Fried[1]*

[1] Department of Chemistry, Johns Hopkins University, Baltimore, Maryland, USA 21218
*To whom correspondence is due: sdfried@jhu.edu

Table of Contents

I. Supplementary Texts. 2
II. Supplementary Methods. 6
III. Supplementary Figures. 14
1. Development of A Coupled Fluorescence for Loopable Translation. . .14
2. Cell Growth Curve. 15
3. Strengthening P6a. 16
4. Installing Flexible Linkers. 17
5. Improving TEV Protease. 18
6. Replacing SD with IRES. 19
7. Design of Ribozyme-based Loopable Translator. 20
8. Northern Blot. 21
9. Loopable Translator Constructs Prepared in Truncation Series. . .22
10. Flow Chart of Constructs. 23
11. The Sequence of pBAD-tdTEVDB. 24
IV. Supplementary Tables. 25
V. Supplementary References. 30

I. Supplementary Texts

1. Installing Extra GC Pairs at P6a. Permutation of the native td intron (Fig. 3A) to create the loopable translator (pBAD-tdTEVDB) impacts P6a by deleting its internal ORF and generating new 5' and 3' termini. We speculated that such a change could have disrupted the native P6a stability[1] and negatively impacted the mRNA circularization of our construct. Thus, to compensate for the potential disruption at P6a stem, we installed a total of 12 extra GC pairs at P6a of pBAD-tdTEVDB (denoted as "pBAD-tdTEVDB-P6a") and quantified the changes in the efficiency of mRNA circularization via a fluorescence-based plate reader assay (Fig. S3B). This actually led to lower activity, suggesting that P6a should not be over-stabilized and that permutation did not disrupt the ability of the two strands (at the 5' and 3' termini of the RNA molecule) to associate to form the P6a helix.

2. Installing Flexible Linker at Upstream and Downstream of RBS. Suboptimal processing of the sfGFP concatemer by TEV protease would mask the fluorescence signals arising from fluorescent monomers that are yet liberated[2–4]. Hence, it is of interest to improve the protease activity to the extent that the GFP chain is fully cleaved into monomers in real-time basis. We hypothesized that TEV protease might have difficulty accessing its cleavage site in pBAD-tdTEVDB due to insufficient flexibility of the neighboring protein sequences. Thus, we decided to install flexible linkers (GGSGGGSGG) at the upstream and downstream of TEV cleavage site in pBAD-tdTEVDB (Fig. S4A) and quantify the change in signals via a fluorescence-based plate

reader assay (Fig. S4B). Additional flexibility proved not to have a beneficial effect, supporting the view that TEV protease activity was not limiting (see also Fig. 4).

3. Modifying TEV Protease. To see if the activity of TEV protease could be improved based on previous work from the literature, we decided to modify the protein sequence based on two examples. Fan and coworkers[5] showed an improved performance of the TEV protease with two point mutations (L56V and S135G) and Ting and coworkers[6] reported another variant which retains the above point mutations and was truncated after residue 219 (Fig. S5A). pBAD-tdTEVDB was used as a construct of choice to compare the activity of the three versions of TEV protease via a fluorescence assay (Fig. S5B). The TEV mutants did not provide a beneficial effect, supporting the view that TEV protease activity was not limiting (see also Fig. 4).

4. Replacing Shine-Dalgarno with Eukaryotic IRES. The bacterial Shine-Dalgarno sequence (aaggag) of pBAD-tdTEVDB was replaced with a viral internal ribosome entry site (IRES) that has been reported to efficiently recruit bacterial ribosomes (Fig. S6A).[7] In particular, Colussi et al. demonstrated that the isolated domain 3 of the *Plautia stali* intestine virus (PSIV) intergenic region (IGR) IRES allows initiation of *E. coli* ribosomes on mRNA with only slightly reduced performance compared to the full-length IRES.[7] To minimize the scar sequence in the polymer product, domain 3 of PSIV IGR IRES was chosen to replace SD in pBAD-tdTEVDB (Fig. S6B). The low but statistically significantly higher fluorescence than background levels is reminiscent to what we found

with pBAD-tdTEVDB-STOP (Figs. 3C, S6C). This finding suggests that initiation *can* occur via this IRES, but that it is challenging for ribosomes to achieve multiple passes, possibly because the intrinsic helicase activity of ribosomal elongation is insufficient to disassemble the stable IRES pseudoknot (which would be required during looping).

5. Design of Ribozyme-based Loopable Translator. Jeffrey and coworkers utilized the self-cleaving P1 and P3 Twister ribozymes to circularize an RNA of interest in mammalian cells.[8] They designed a transcript that transcribes a region to be circularized flanked by the two self-cleaving ribozymes which form a 5'-OH and a 2',3' -cyclic phosphate at the 3' terminus. The resulting termini undergo a direct ligation by the RNA ligase, RtcB, that completes a tRNA splicing process in eukaryotes.[9,10] Later studies discovered that bacterial, archaeal, and mammalian RtcBs are all capable of directly ligating the 5' hydroxyl and 2', 3' -cyclic phosphate termini.[11–14] The *E. coli* genome has an ortholog of RtcB, which is not expressed under most conditions (*E. coli* also has no tRNAs that require splicing).[15,16] Upon over-expression, *E. coli*'s RtcB has been demonstrated to be active in tRNA ligation.[15] Hence, we designed a ribozyme-based loopable translator in which the permuted sfGFP was flanked by tRNA context sequences (orange) and P1 and P3 ribozymes (blue) as in ref. 8 (Fig. S7A). This construct also overexpresses *E. coli* RtcB in trans, owing to the fact that the endogenous copy is not expressed. The fluorescence signals arising from this construct was very low, though still significantly above baseline levels (Fig. S7B). These results are inconsistent with the efficiency reported by the authors of ref. 8; we suggest that

RtcB-based ligation may be more efficient in eukaryotic cells than in bacteria. It is also possible that sequence changes to the pairing regions to mimic *E. coli* $tRNA_{Tyr}$ (see Fig. S7A and Table S1) lowered the efficiency of the enzymatic ligation.

II. Supplementary Methods

Cell Growth Curve. To test for possible toxicities associated with loopable translation, three constructs corresponding to negative control, positive control, and pBAD-tdTEVDB were transformed into BL21+pRK793 cells (with TEV protease) and grown as described in the main text. Three separate colonies were inoculated into 3x200 uL of LB media supplemented with ampicillin, tetracycline, 0.2% arabinose, and 20 mM Mg^{2+} in a clear-bottom 96-well plate (Costar) and expressed at 30 °C. With the starting OD_{600} of 0.05, the growth was measured in every 10 min over the course of 16 hours (Fig. S2). We found no significant difference in growth rates across these three strains.

Installing Extra GC Pairs at P6a. A total of 12 extra GC basepairs were installed at P6a of pBAD-tdTEVDB by PCR and Gibson assembly. The backbone was linearized with primers BB-P6a-F and BB-P6a-R and the insert was prepared with primers Insert-P6a-F and Insert-P6a-R (Figs. S3, S10; Table S1). PCR products were size-verified by 0.8% agarose gel electrophoresis, digested with DpnI, column purified, combined with each other and 2X Hi-Fi reaction mixture (following the manufacturer's protocol), and transformed into 10-beta cells as described in the main text. The plasmid was sequence verified, before transformed into BL21(DE3)+pRK793 cells, and assessed using the fluorescence assay method described in the main text.

Installing Flexible Linker at Upstream and Downstream of RBS. Flexible linkers (GGSGGGSGG) were installed at upstream and downstream of the TEV cleavage site in pBAD-tdTEVDB with primers flexiTEV-F and flexiTEV-R via QuickChange (Figs. S4, S10; Table S1). The PCR product was size-verified by 0.8% agarose gel electrophoresis, digested with DpnI, column purified, and transformed into 10-beta cells as described in the main text. The plasmid was sequence verified, before transformed into BL21(DE3)+pRK793 cells, and assessed using the fluorescence assay method described in the main text.

Modifying TEV Protease. The pRK793 plasmid containing a gene that encodes a soluble form of TEV protease (241 AA)[17,18] was obtained as a gift from Barrick laboratory (JHU Biophysics department). Using the plasmid as the template, a TEV protease variant carrying two-point mutations (L56V and S135G) was made by PCR via two consecutive QuickChanges using primers TEVP_BB_F2 and TEVP_Fragment_R, and then TEVP_BB_F and TEVP_BB_R (denoted as "DM") (Figs. S5A, S10; Table S1). A second variant of TEV protease was made by truncating after residue 219 in the double mutant background (denoted as "TEVP2_Delta"). Using TEVP_L56V+S135G as the template, the second variant was made by PCR with primers TEVP_BB_F2/R2. The three versions of TEV proteases were sequence-verified, transformed into BL21(DE3), and the cells were made competent again (as described in the main text) to generate three strains of competent cells: BL21(DE3)+pRK793 (original TEV protease), BL21(DE3)+pRK793_DM (with L56V+S135G), and BL21(DE3)+pRK793_TEVP2 (with

L56V+S135G and truncation). These cells were then transformed with pBAD-tdTEVDB, and fluorescence from each was measured via a plate reader assay as described in the main text (Fig. S5B). The variants of TEVP did not result in significant differences in fluorescence activity.

Replacing Shine-Dalgarno with Eukaryotic IRES. A construct with IRES-based initiation was made by Gibson assembly. The insert was amplified by PCR out of a separate previously constructed plasmid containing the IRES domain 3 sequence (pYES_td_2A_FP_IRES_2A_P) with primers IRES_Domain3_F and IRES_R2 (Figs. S6A-B, S10; Table S1). The insert was then ligated into a linearized pBAD backbone that was made from pBAD-tdTEVDB by PCR with primers IRES_TEVDB_BB_F/R (Figs. S6A-B, S10; Table S1). The plasmid was sequence-verified and then transformed into BL21(DE3)+pRK793. Fluorescence was measured via a plate reader assay as described in the main text (Fig. S6C). This construct generated signal close to baseline levels.

Replacing td intron with P1 and P3 Twister Ribozyme Sequences. An extra copy of *E. coli* RtcB was installed downstream of the tetracycline efflux protein (TetR) of pBAD-tdTEVDB via Gibson assembly in which a linearized pBAD backbone was made by PCR with primers pBAD_BB_RtcB_F/R and the insert was made by PCR with primers RtcB_F/R using *E. coli* chromosomal DNA as a template (Fig. S7A; Table S1). Then the RtcB-containing pBAD-tdTEVDB was linearized by PCR with primers pBAD-BB_2_F/R and ligated via Gibson assembly with a geneBlock (“Ribozyme”; Table S1)

that was ordered from IDT. The plasmid was sequence-verified and then transformed into BL21(DE3)+pRK793. Fluorescence was measured via a plate reader assay as described in the main text (Fig. S7B). This construct generated signal close to baseline levels.

Northern Blot. The negative control (pBAD-sfGFP$_{1-52}$) and pBAD-tdTEVDB were transformed into BL21 and expressed at 30 °C in LB media supplemented with Tetracycline, 0.2% arabinose, and 20 mM $MgCl_2$. With a starting OD_{600} of 0.05, the cell cultures were grown to OD_{600} of 1.0~1.2, and centrifuged at 5,000 rpm for 15 min at 4 °C to generate cell pellets. Total RNAs were extracted from the cell pellets via Trizol extraction methods followed by the manufacturer's protocol (Invitrogen). The extracted RNAs were resuspended in 50 μL of DEPC-treated water and measured for concentrations using NanoDrop.

Approximately 3 μg of the extracted RNAs were mixed with 9 uL of 2X of RNA dye (NEB) via vortexing, denatured at 70 °C for 20 min, and separated by native electrophoresis with a 4% TBE-acrylamide gel using 0.5X TBE buffer at 180 V for 45 min at room temperature. The separated RNAs were electroblotted to a nylon membrane using iBlot2 (7 min; 20 V) and immobilized using "Auto Cross Link" mode of UV Stratalinker 1800 (Strategen). The fixed nylon blot was preincubated in a pre-heated hybridization buffer (UltraHyb buffer; Invitrogen) for 30 min at 42 °C. Then a biotinylated DNA probe which was designed to anneal to RNA sequences corresponding to GFP residue 58 to 66 (present in the circularized loop generated by pBAD-tdTEVDB; Table

S1) was added to the hybridization buffer to a final concentration of 100 pM, and the blot was hybridized overnight at 42 °C. The blot was washed 2x 5 min in Ambion NorthernMax™ Low Stringency Wash Buffer #1 (Invitrogen) and again washed 2x 15 min in Ambion NorthernMax™ High Stringency Wash Buffer #2 (Invitrogen).

To block the nylon blot, the blot was incubated in 16 mL of 1X I-Block blocking buffer (1X PBS, 0.5% SDS, 0.1% I-Block Protein-Based Blocking Reagent (Invitrogen)) for 15 min at room temperature with a gentle shaking. Streptavidin-Horseradish Peroxide conjugate (Thermo Scientific) was added to the blocking buffer to a final concentration of 0.3 ug/mL, and the blot was incubated for 15 min with a gentle shaking. Then the nylon membrane was washed 4x 5 min each with 20 mL of 1X wash buffer (1X PBS, 0.5% SDS) with a gentle shaking. After the washing, the nylon blot was incubated for 5 min in 8 mL mixture of SuperSignal™ West Pico Plus Chemiluminescent Substrates (mixed in a 1:1 ratio; Thermo Scientific) and taken image using ChemiDoc Touch Imaging System (BioRad).

Creation of the Context Truncation Series. Truncations and modifications of the 5' and 3' td exon context sequences were generated through QuickChange. Various primers (see Table S1, Fig. S9 & S10 for details and sequences) were used in PCR reactions with pBAD-tdTEVDB as a template. PCR products were size-verified by 0.8% agarose gel electrophoresis, digested with DpnI, column purified, and transformed into 10-beta cells as described previously. All plasmids were sequence verified, before

transforming them into BL21(DE3)+pRK793 cells, and assessed using the fluorescence assay method described in the main text.

Creating Constructs with Tandem Dragline Silk Multimers. A minigene plasmid (entitled "pIDT-silk-unit") containing a flexible tag, part of MaSp1 sequence (dragline silk), and a His(6)-tag (Table S1) was ordered from IDT, and the above sequence of interest was amplified via PCR using primers Amp_silk_repetitive_unit_F and Gib_silk_tandem_seq_R (Table S1). The resulting PCR product has a recognition site for NheI between the flexible tag and the MaSp1 and a recognition site for SpeI between the MaSp1 and the His-tag, enabling a directional cloning in the downstream synthesis of constructs for tandem silk multimers. The PCR product was checked on 0.8% agarose gel, DpnI digested, and column-purified as previously described, and digested with NheI and SpeI. Then the silk insert was ligated back in a head-to-tail fashion into pIDT-silk-unit plasmid that was digested only with either NheI or SpeI (Fig. 1).[1,6] A successful ligation removes the recognition site between the two silk-mers, generating a plasmid that has a tandem silk dimer.[1,6] The above strategy was used to make three pIDT constructs containing tandem silk multimers in different lengths (silk 8-mer, 16-mer, and 24-mer). The synthesized silk multimers were excised from the above pIDT constructs using NheI and SpeI, separated by 0.8% agarose gel, and gel-purified using QIAquick Gel Extraction Kit (QIAGEN). For non-looped silk multimer constructs, pBAD-sfGFP plasmid was used as a template to generate a linearized pBAD backbone by PCR using linearize_F/R (Table S1). Following PCR, the linearized pBAD backbone

obtained recognition sites for AvrII and SpeI at the 5' and 3' end, respectively. The pBAD backbone was first digested with AvrII and SpeI, dephosphorylated, and then ligated with each of the silk multimer inserts that were digested with NheI and SpeI.[1,6] For looped silk multimer constructs, the pBAD backbone was generated by PCR with primers TEVDB_Pemuted_F/R (Table S1) using pBAD-tdTEVDB with only 6 exonic context sequence on its 3' end (Fig. 5E) as a template. The linearized pBAD backbone also has the recognition sites for AvrII and SpeI at each end, then was digested with AvrII and SpeI, dephosphorylated, and then ligated with each of the silk multimer inserts that were digested with NheI and SpeI. All six ligated products were transformed into 10-beta competent cells, and processed as described previously, resulting in three non-looped pBAD constructs and three looped pBAD constructs containing silk 8-mer, 16-mer, and 24-mer (Fig. 7A). The synthesized six constructs were verified by Sanger Sequencing.

Protein Expression and Western Blot of Silk Constructs. For expression, the six constructs with silk multimers were transformed into BL21(DE3) as previously described, and 40 μL of the transformants were spread out on selective plates with LB agar supplemented with 15 μg/ml tetracycline. The plates were incubated at 37˚C overnight (~16h), and one colony of each plate was picked with sterile pipette tips and inoculated in 5 mL of LB supplemented with 15 μg/ml tetracycline to make overnight cultures which were incubated at 37˚C overnight with agitation (220 rpm). The overnight cultures were then used to start day cultures in 50 mL of LB supplemented with 7.5

μg/ml tetracycline, 0.2% arabinose and 20 mM $MgCl_2$ at a starting OD_{600} of 0.05. The day cultures were incubated at 30˚C overnight with agitation (220 rpm), and cells from 1 mL aliquots were collected by centrifugation at 4˚C at 3000 *g* for 20 min and stored at -20˚C until future use.

Frozen cell pellets were thawed on ice for 15 min, resuspended with 500 μL of lysis buffer (1 mM Tris-HCl, pH 8.0, 20 mM NaH_2PO_4, 8 M Urea, 2 M thiourea; Table S2), and incubated at room temperature overnight (~16h) with inversion (50 rpm, Roto-mini rotator). 24 μL of the resulting lysates were mixed with 6 μL of 5X Tris-Glycine-SDS loading buffer via vortexing. The samples were not heated and directly loaded onto pre-cast Novex WedgeWell 8% Tris-glycine gels with 3 μL of Pre-stained PAGE ruler as the ladder (ThermoFisher Scientific; #26619). The rest of the western was performed as previously described, using diluted anti-His primary antibody (Invitrogen) and anti-mouse-HRP secondary antibody (Invitrogen). The incubated membrane was rinsed as previously described, developed in chemiluminescence reagents (Signal West Femto Maximum Sensitive Substrate; ThermoFisher Scientific), and images were acquired using a Chemi-Doc imager (BioRad).

III. Supplementary Figures

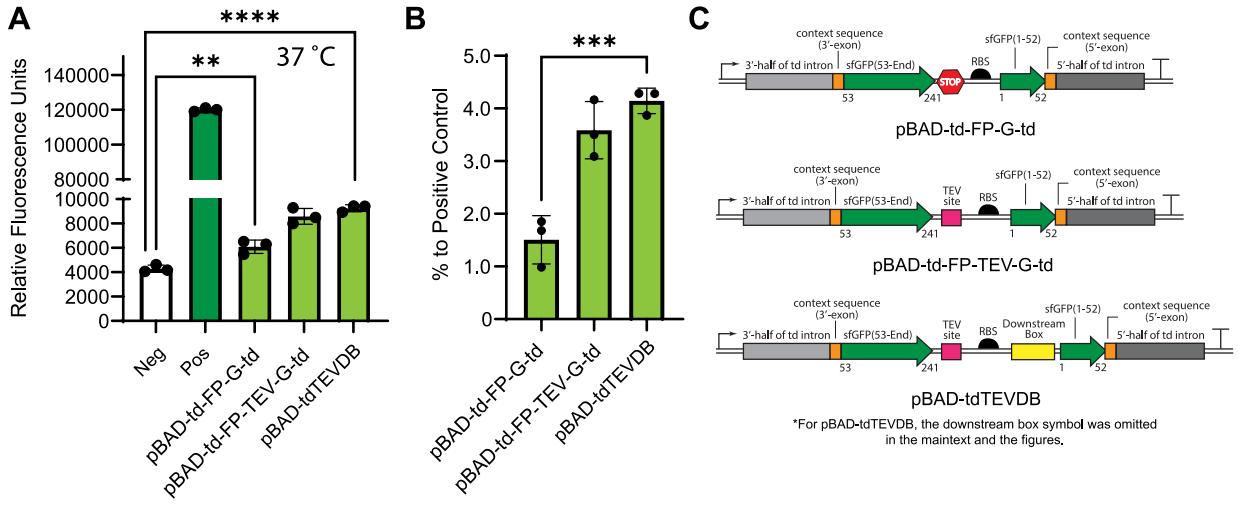

Figure S1. Development of A Coupled Fluorescence for Loopable Translation. (**A**) Bar chart showing the level of fluorescence of the controls, prototypes, and loopable translator. The original construct, td-FP-G-td (see Methods), generated signal that is only slightly higher than baseline (P value = 0.0075 by Student's t-test). pBAD-tdTEVDB generated signal that is significantly higher than the baseline (P value < 0.0001 by Student's t-test) (**B**) Bar chart showing the relative performance of the same set of constructs compared to the positive control following background subtraction. pBAD-tdTEVDB generated significantly higher fluorescence compared to the prototype td-FP-G-td design (2.8-fold, P-value = 0.0009 by Student's t-test). (**C**) Constructs designed for the loopable translation.

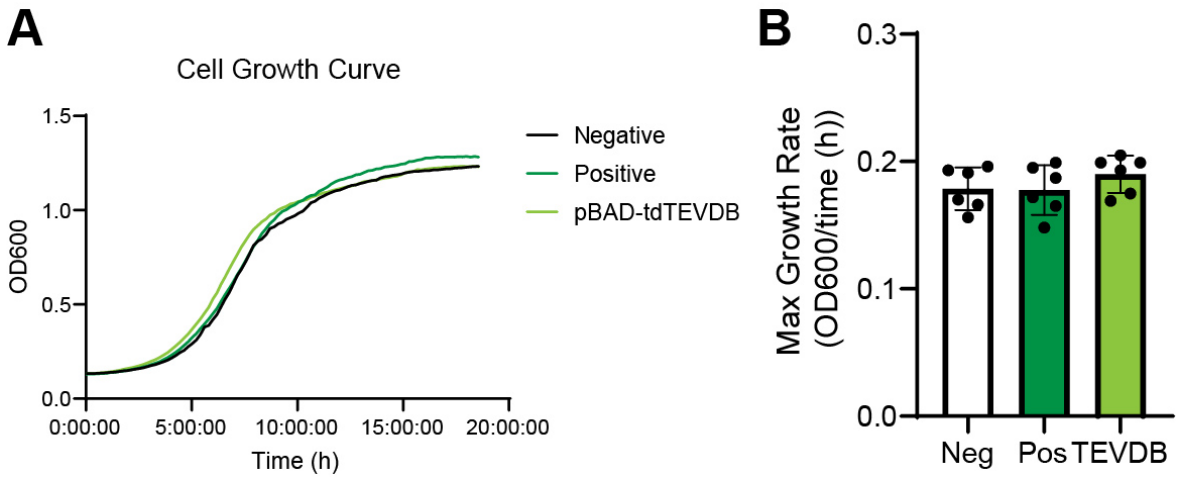

Figure S2. Cell Growth Curve (**A**) Negative control, positive control, and pBAD-tdTEVDB were expressed in BL21+pRK793 and grown at 30 °C in a 96 well plate as OD_{600} was measured in every 10 min over the course of 16h. BL21+pRK793 harboring each of the three constructs were inoculated in LB media supplemented with antibiotics (ampicillin and tetracycline), IPTG (0.1mM), arabinose (0.2%), and 20 mM Mg^{2+} to staring ODs of 0.05. (**B**) Bar chart showing the growth rates of the above constructs. No significant difference in growth rates was observed for the samples, indicating that there is no cell toxicity caused by loopable translation of pBAD-tdTEVDB.

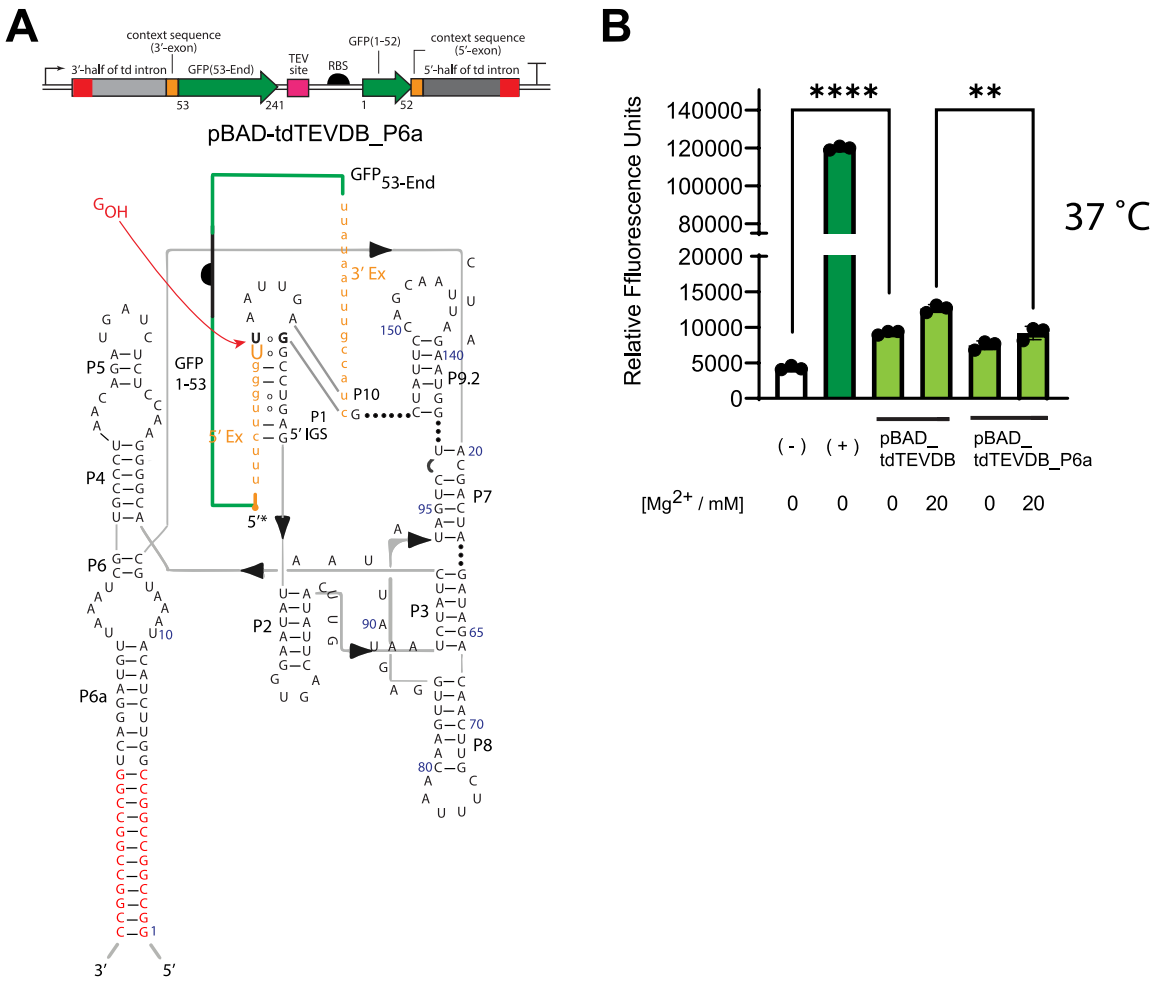

Figure S3. A Rational Approach to Improve Loopable Translator: Strengthening p6a. (**A**) Secondary structure of the P6a-modified construct (pBAD-tdTEVDB-P6a). Upon DNA permutation to make pBAD-tdTEVDB, the native td intron was cleaved at P6a, creating new 5' and 3' termini in the place of P6a ORF. To compensate the potentially destabilized P6a, a total of 12 extra GC pairs were installed to strengthen the structure. (**B**) Bar chart showing the level of fluorescence of pBAD-tdTEVDB and pBAD-tdTEVDB-P6a with different concentrations of $MgCl_2$. Additional GC pairs at P6a decreased the activity of the loopable translator (0.73-fold, P-value = 0.005 by Student's t-test).

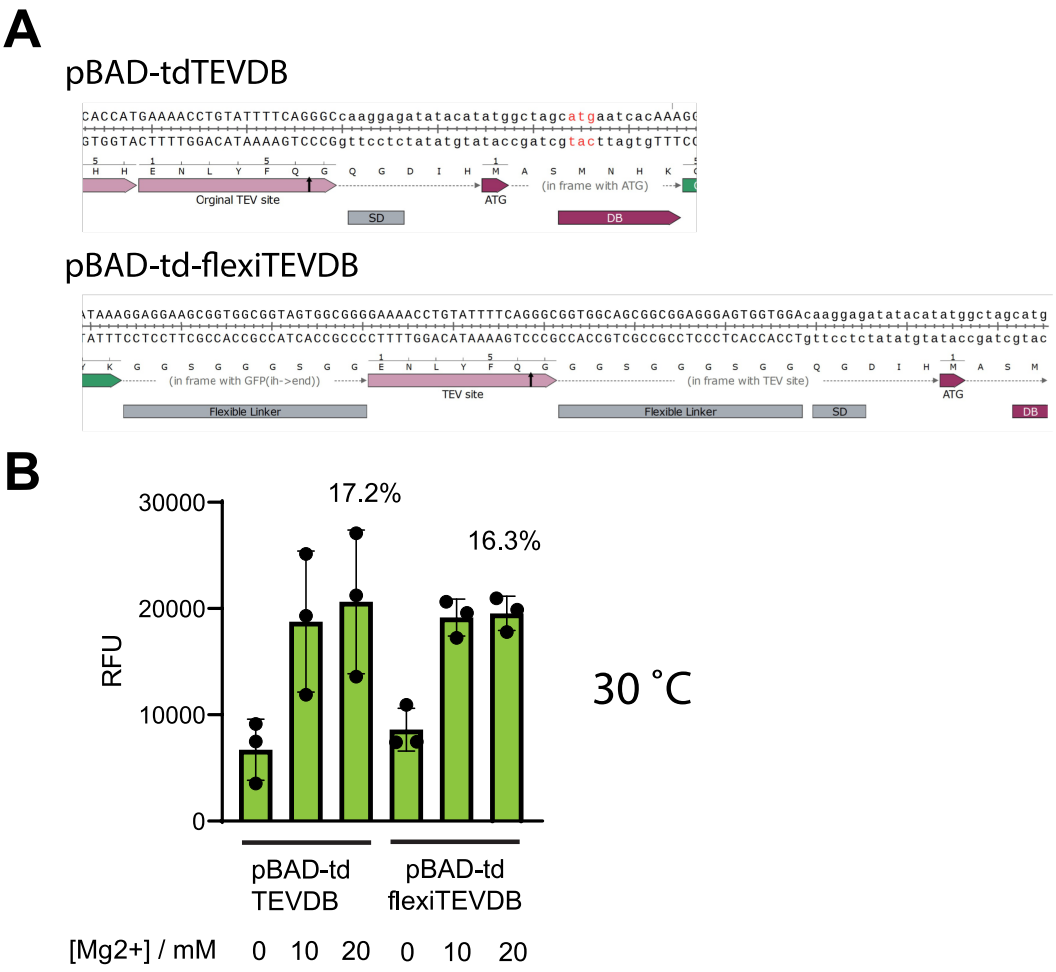

Figure S4. A Rational Approach to Improve Loopable Translator: Installing Flexible Linkers. (**A**) Illustration of pBAD-tdTEVDB and a new construct (pBAD-td-flexiTEVDB) that has flexible linkers (GGSGGGSGG) at the upstream and downstream of TEV cleavage site. (**B**) Bar chart showing the level of fluorescence of pBAD-tdTEVDB and pBAD-td-flexiTEVDB with different concentrations of $MgCl_2$. Additional flexibility in the neighboring sequences of TEV cleavage site had no significant effect on improving the fluorescence signal of pBAD-tdTEVDB.

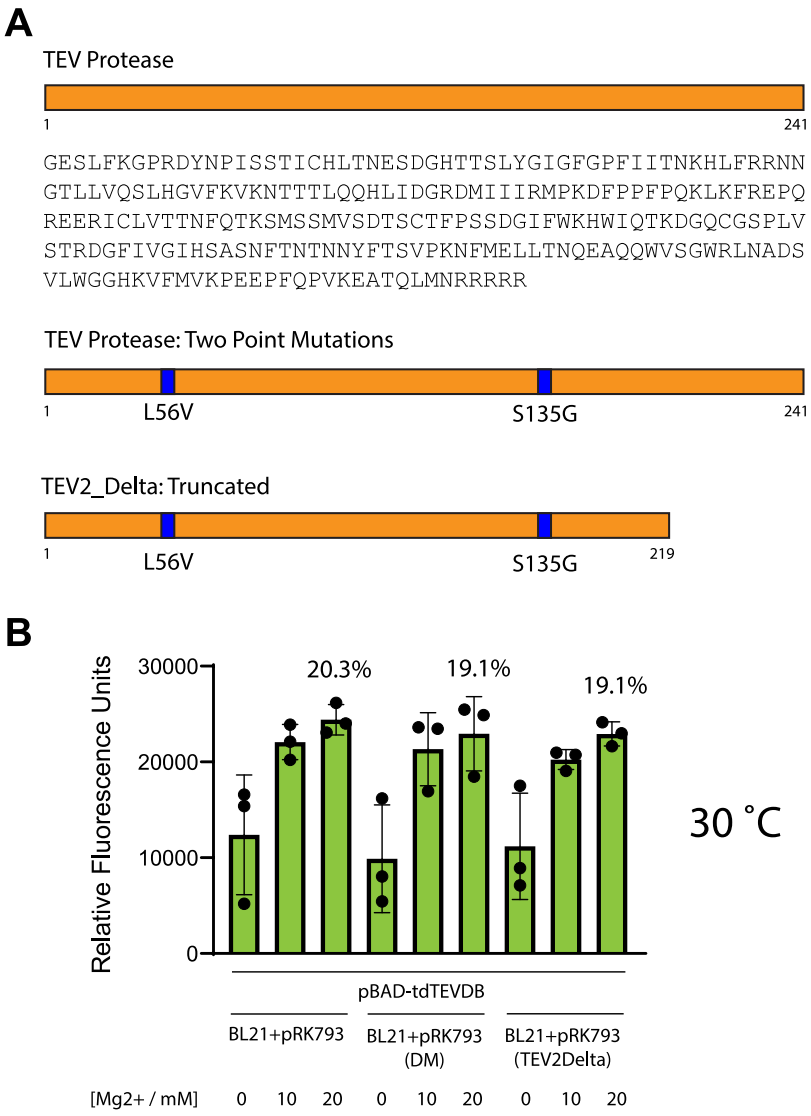

Figure S5. A Rational Approach to Improve Loopable Translator: Improving TEV Protease. (**A**) Illustration of three different versions of TEV protease: the 'original' TEV protease (reported by Waugh and co-workers) was either modified with two point mutations (L56V/S135G; ref. 5) or truncated after residue 219 with the same two point mutations (ref. 6). (**B**) Bar chart showing the level of fluorescence at 30˚C associated with the three different TEV proteases. The difference in the fluorescence level was not significant (Student's t-test).

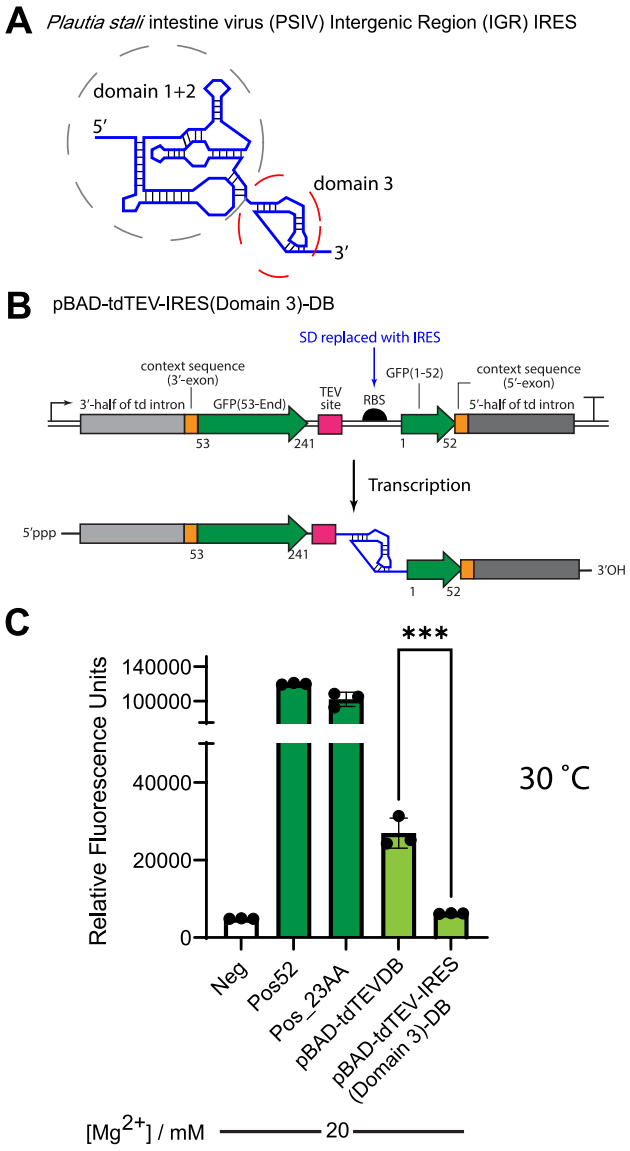

Figure S6. A Rational Approach to Improve Loopable Translator: Replacing SD with IRES. (**A**) Illustration of *Plautia stali* intestine virus (PSIV) intergenic region (IGR) IRES. PSIV IGR IRES is a eukaryotic IRES that was found to initiate translation in bacteria (*E. coli*; ref. 7). Domain 3 of PSIV IGR IRES was also found to solely initiate translation in *E. coli* with slightly reduced performance compared to its wildtype. (**B**) Illustration of SD replacement with PSIV IGR IRES. (**C**) Bar chart showing the level of fluorescence of a set of constructs (negative control, positive control, new positive control with 23AA scar sequence, pBAD-tdTEVDB, and pBAD-tdTEV-IRES (Domain 3)-DB) at 30°C with 20 mM $MgCl_2$. The IRES construct produced signal that was slightly higher than baseline levels (1.3-fold, $P < 0.0001$ by Student's t-test), nevertheless its performance was 4.3-fold reduced relative to the intron-based loopable translator ($P=0.0007$ by Student's t-test).

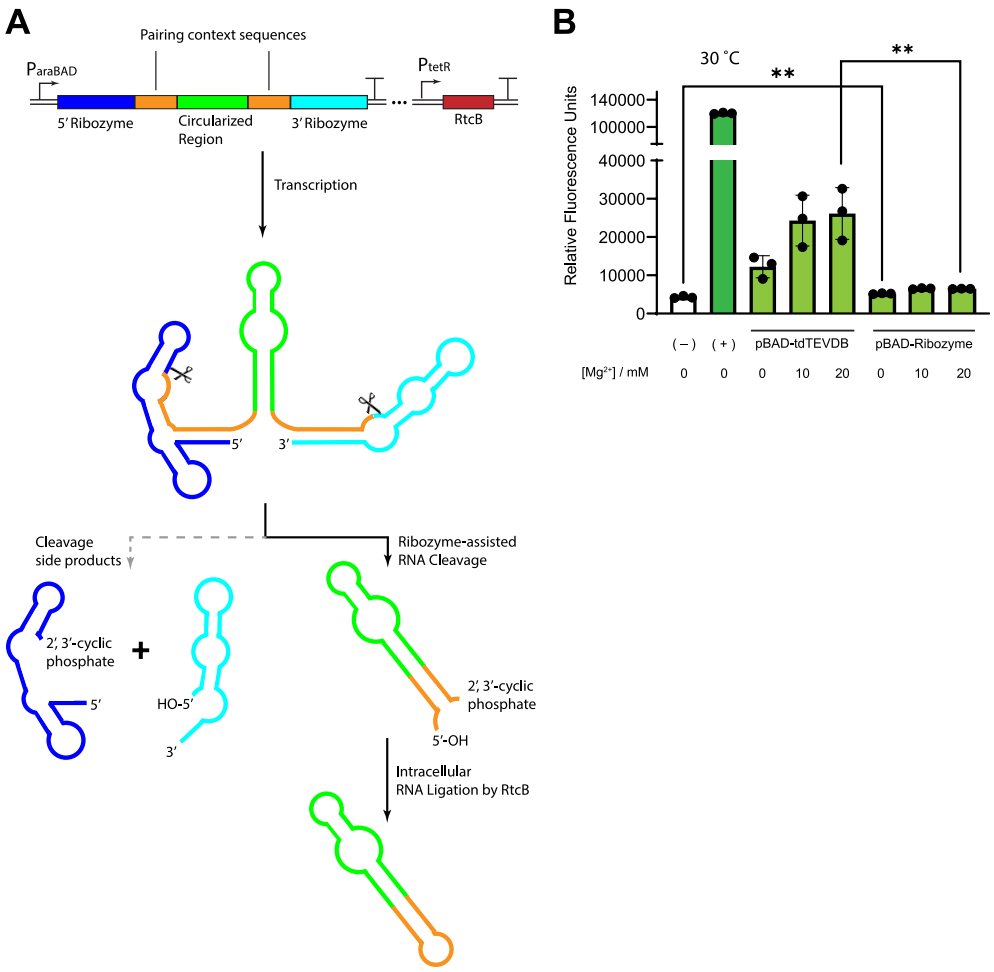

Figure S7. Design of Ribozyme-based Loopable Translator. (**A**) Illustration of the DNA sequence for ribozyme-based loopable translator (pBAD-Ribozyme; ref. 8). In this design, a region to be circularized (green) is inserted between two self-cleaving ribozyme sequences (dark and light blue). The cleavage results in a 5'-OH and 2',3-'cyclic phosphate termini. In the context of a tRNA molecule, these termini are ligated by the enzyme RtcB. Hence, in the ribozyme-based looping strategy, a region to be circularized is flanked with tRNA context sequences (orange) creating the sequence and end modifications that would be recognized by RtcB. (**B**) Bar chart showing the level of fluorescence of a set of constructs (negative control, positive control, pBAD-tdTEVDB, and pBAD-Ribozyme) at 30°C with varying concentrations of $MgCl_2$. Although pBAD-Ribozyme generated signal that was significantly higher than the baseline (1.2-fold, P=0.0086 by Student's t-test), it generated 4-fold less signal compared to pBAD-tdTEVDB (P=0.0073 by Student's t-test).

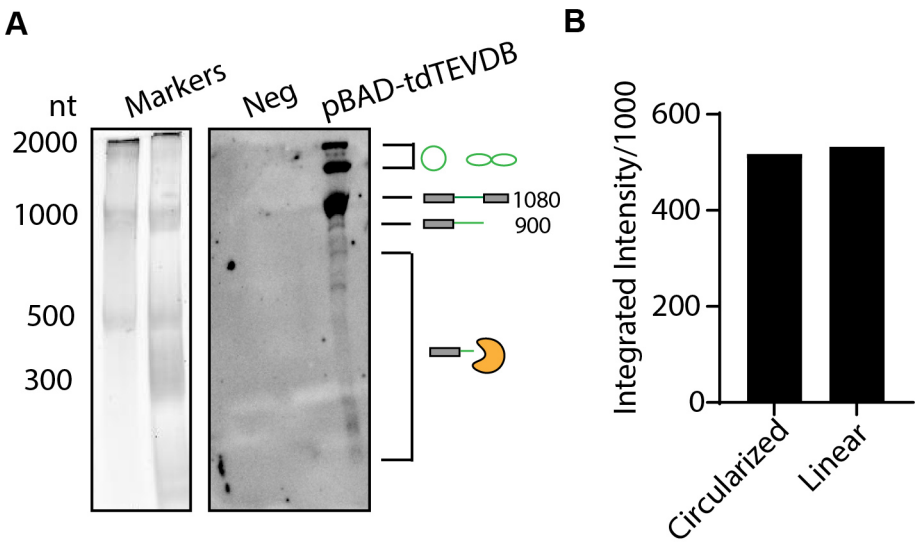

Figure S8. Northern Blot. (**A**) A Northern blot image showing the RNA products generated from the negative control (pBAD-sfGFP$_{1\text{-}52}$) and pBAD-tdTEVDB. A biotinylated DNA probe (Table S1) was designed to anneal to RNA sequences corresponding to GFP residue 58 to 66 (present in the circularized loop generated by pBAD-tdTEVDB). Two ssRNA markers (ssRNA ladder (NEB); Low Range ssRNA ladder (NEB)) separated by electrophoresis under the identical condition to that of the Northern blot were used to estimate the size of the RNA bands. The linear RNA product prior to the autocatalytic cleavage is 1080 nt long, and the ribozymic intermediate is expected to be 900 nt long. Circular RNA is known to have significantly *lower* electrophoretic mobility (cf. refs. 2 & 4), allowing us to assign high apparent-MW bands to circRNA. The lower of the two is tentatively assigned to a single supercoil. Low MW bands are presumed to be partial degradation products. (**B**) Densitometry of panel A, showing relative integrated intensities of the circularized and linear RNA products.

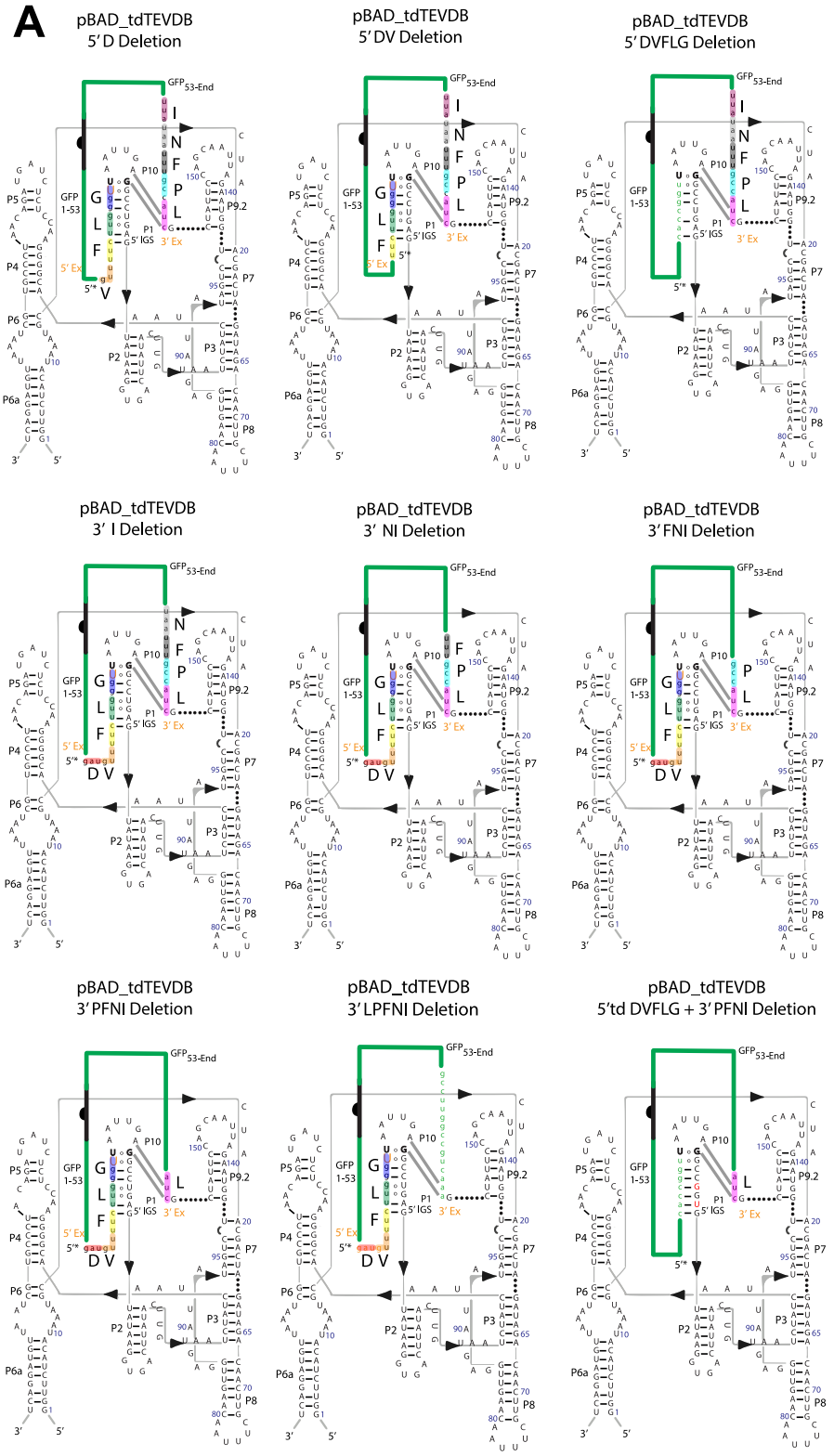

Figure S9. Illustration of Loopable Translator Constructs Prepared in Truncation Series.

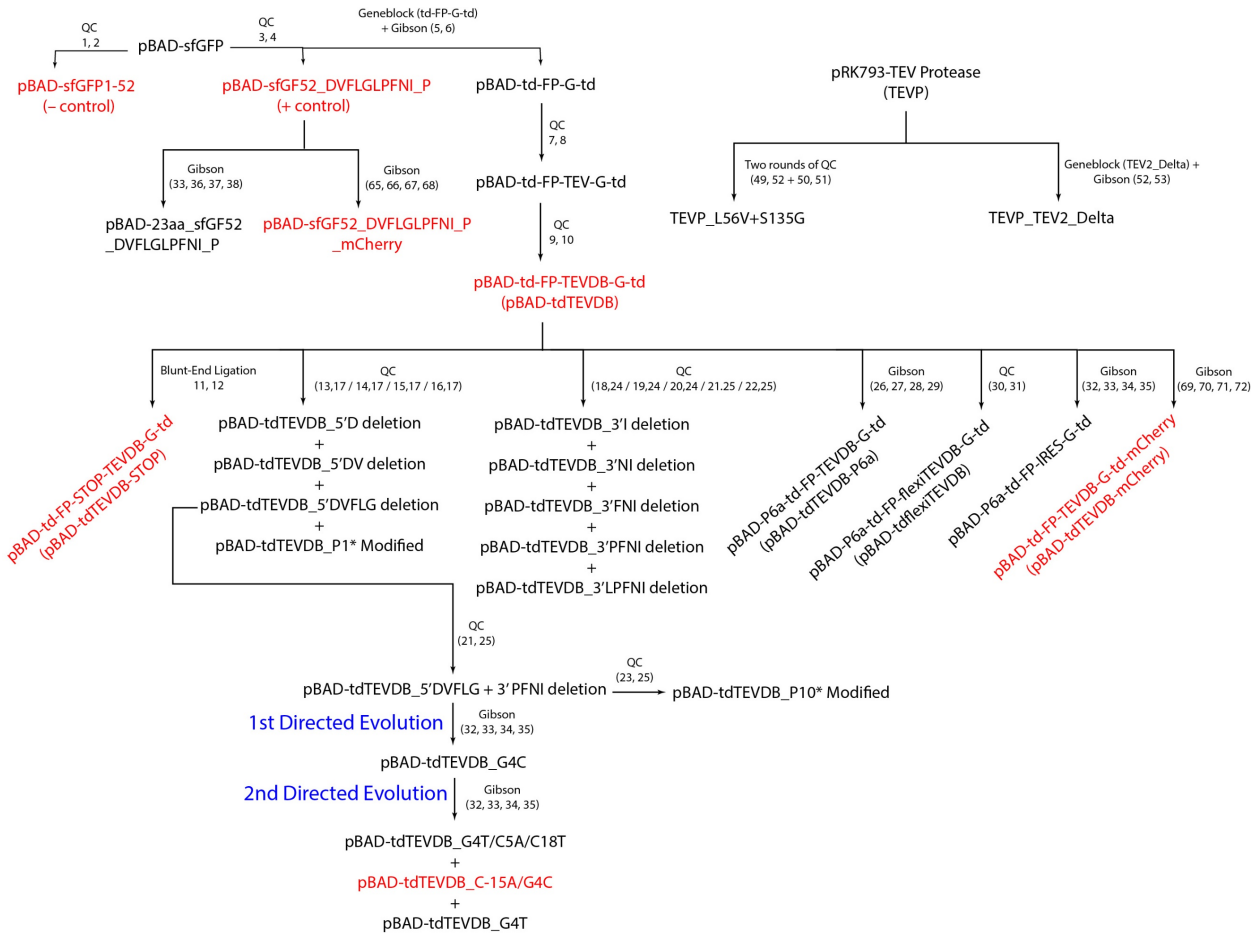

Figure S10. Flow Chart of Constructs. A full list of synthesized constructs and primers along with the process on how each construct was made.

>sequence of pBAD-tdTEVDB

gaattggttctacataaatgcctaacgactatccctttggggagtagggtcaagtgactcgaaa
cgatagacaacttgctttaacaagttggagatatagtctgctctgcatggtgacatgcagctgg
atataattccggggtaagattaacgaccttatctgaacataatgCTACCGTTTAATATTAAACT
GCCGGTTCCGTGGCCGACCCTGGTGACCACCCTGACCTATGGCGTTCAGTGCTTTAGCCGCTAT
CCGGATCATATGAAACGCCATGATTTCTTTAAAAGCGCGATGCCGGAAGGCTATGTGCAGGAAC
GTACCATTAGCTTCAAAGATGATGGCACCTATAAAACCCGTGCGGAAGTTAAATTTGAAGGCGA
TACCCTGGTGAACCGCATTGAACTGAAAGGTATTGATTTTAAAGAAGATGGCAACATTCTGGGT
CATAAACTGGAATATAATTTCAACAGCCATAACGTGTATATTACCGCCGATAAACAGAAAAATG
GCATCAAAGCGAACTTTAAAATCCGTCACAACGTGGAAGATGGTAGCGTGCAGCTGGCGGATCA
TTATCAGCAGAATACCCCGATTGGTGATGGCCCGGTGCTGCTGCCGGATAATCATTATCTGAGC
ACCCAGAGCGTTCTGAGCAAAGATCCGAATGAAAAACGTGATCATATGGTGCTGCTGGAATTTG
TTACCGCCGCGGGCATTACCCACGGTATGGATGAACTGTATAAAGGCAGCCACCATCATCATCA
CCATGAAAACCTGTATTTTCAGGGCcaaggagatatacatatggctagcatgaatcacAAAGGT
GAAGAACTGTTTACCGGCGTTGTGCCGATTCTGGTGGAACTGGATGGTGATGTGAATGGCCATA
AATTTAGCGTTCGTGGCGAAGGCGAAGGTGATGCGACCAACGGTAAACTGACCCTGAAATTTAT
TTGCACCACCGGTGATGTTTTCTTGGGTtaattgaggcctgagtataaggtgacttatacttgt
aatctatctaaacggggaacctctctagtagacaatcccgtgctaaattgtaggact

grey (beginning) = 3' half of td intron. ORANGE = td 3'-exon context sequence. GREEN = GFP(53 to end). PINK = TEV site. Dark grey = SD sequence (RBS). LIME = GFP(1 to 52).
UMBER = td 5'-exon context sequence. grey (end) = 5' half of td intron

>sequence of pBAD-tdTEVDB following context reduction + directed evol of RBS

gaattggttctacataaatgcctaacgactatccctttggggagtagggtcaagtgactcgaaa
cgatagacaacttgctttaacaagttggagatatagtctgctctgcatggtgacatgcagctgg
atataattccggggtaagattaacgaccttatctgaacataatgCTAAAACTGCCGGTTCCGTG
GCCGACCCTGGTGACCACCCTGACCTATGGCGTTCAGTGCTTTAGCCGCTATCCGGATCATATG
AAACGCCATGATTTCTTTAAAAGCGCGATGCCGGAAGGCTATGTGCAGGAACGTACCATTAGCT
TCAAAGATGATGGCACCTATAAAACCCGTGCGGAAGTTAAATTTGAAGGCGATACCCTGGTGAA
CCGCATTGAACTGAAAGGTATTGATTTTAAAGAAGATGGCAACATTCTGGGTCATAAACTGGAA
TATAATTTCAACAGCCATAACGTGTATATTACCGCCGATAAACAGAAAAATGGCATCAAAGCGA
ACTTTAAAATCCGTCACAACGTGGAAGATGGTAGCGTGCAGCTGGCGGATCATTATCAGCAGAA
TACCCCGATTGGTGATGGCCCGGTGCTGCTGCCGGATAATCATTATCTGAGCACCCAGAGCGTT
CTGAGCAAAGATCCGAATGAAAAACGTGATCATATGGTGCTGCTGGAATTTGTTACCGCCGCGG
GCATTACCCACGGTATGGATGAACTGTATAAAGGCAGCCACCATCATCATCACCATGAAAACCT
GTATTTTCAGGGCaaaggagatatacatatgCctagcatgaatcacAAAGGTGAAGAACTGTTT
ACCGGCGTTGTGCCGATTCTGGTGGAACTGGATGGTGATGTGAATGGCCATAAATTTAGCGTTC
GTGGCGAAGGCGAAGGTGATGCGACCAACGGTAAACTGACCCTGAAATTTATTTGCACCACCGG
Ttaattgaggcctgagtataaggtgacttatacttgtaatctatctaaacggggaacctctcta
gtagacaatcccgtgctaaattgtaggact

ORANGE = reduced td 3'-exon context sequence. Red = mutations to initiation region from directed evolution. UMBER = reduced td 5'-exon context (see text as GFP sequence participates)

Figure S11. The sequence of pBAD-tdTEVDB before and after optimization with annotations shown in color.

IV. Supplementary Tables

Table S1. All Primers, GeneBlocks, and Mini-Gene Sequences Used in This Study

Primers			
	Name	**Length (bp)**	**Sequences (5' to 3')**
1	Delete53-f	42	AATTTATTTGCACCACCGGTTAAAGCTCGAGCGAAGCTTGGG
2	Delete53-r	26	ACCGGTGGTGCAAATAAATTTCAGGG
3	TD_Context_Insert-f	44	TTTCTTGGGTCTACCGTTTAATATTAAACTGCCGGTTCCGTGGC
4	TD_Context_Insert-r	50	TAAACGGTAGACCCAAGAAAACATCACCGGTGGTGCAAATAAATTTCAGG
5	clone-pBADGFP-f	22	GTCTCCCCATGCGAGAGTAGGG
6	clone-pBADGFP-r	33	ATGGAGAAACAGTAGAGAGTTGCGATAAAAAGC
7	TEV-F	45	GAAAACCTGTATTTTCAGGGCCAGGAGGAATTAACCATGGTTAGC
8	TEV-R	43	GCCCTGAAAATACAGGTTTTCATGGTGATGATGATGGTGGCTG
9	InsertDB-F	55	AAGGAGATATACATATGGCTAGCATGAATCACAAAGGTGAAGAACTGTTTACCGG
10	InsertDB-R	46	AGCCATATGTATATCTCCTTGGCCCTGAAAATACAGGTTTTCATGG
11	TEV_DB_STOP_F	29	TAAGAAAACCTGTATTTTCAGGGCCAAGG
12	TEV_DB_STOP_R	23	ATGGTGATGATGATGGTGGCTGC
13	5'td_Delete_D-F	49	ATTTGCACCACCGGTGTTTTCTTGGGTTAATTGAGGCCTGAGTATAAGG
14	5'td_Delete_DV-F	46	ATTTGCACCACCGGTTTCTTGGGTTAATTGAGGCCTGAGTATAAGG
15	5'td_Delete_DVFLG-F	37	ATTTGCACCACCGGTTAATTGAGGCCTGAGTATAAGG
16	5'td_td intron modify-F	71	ATTTGCACCACCGGTTAATTGAGGCCGGTGTATAAGGTGACTTATACTTGTAATCTATCTAAACGGGGAAC
17	5'td_Delete-R	25	ACCGGTGGTGCAAATAAATTTCAGG
18	3'td_Delete_I-F	39	AACATAATGCTACCGTTTAATAAACTGCCGGTTCCGTGG
19	3'td_Delete_NI-F	36	AACATAATGCTACCGTTTAAACTGCCGGTTCCGTGG
20	3'td_Delete_FNI-F	33	AACATAATGCTACCGAAACTGCCGGTTCCGTGG
21	3'td_Delete_PFNI-F	36	TATCTGAACATAATGCTAAAACTGCCGGTTCCGTGG
22	3'td_Delete_LPFNI-F	34	TATCTGAACATAATGAAACTGCCGGTTCCGTGGC
23	3'CUC_F	36	TATCTGAACATAATGCTCAAACTGCCGGTTCCGTGG
24	3'td_Delete-R	33	CGGTAGCATTATGTTCAGATAAGGTCGTTAATC
25	3'td_Delete_R2	33	CATTATGTTCAGATAAGGTCGTTAATCTTACCC
26	BB-P6a-F	33	GGCCGGCCGGCCATGCATATCCTTAGCGAAAGC
27	BB-P6a-R	39	GTAGAACCGGCCGGCCGGCCAATTCGAATTCAGCGTAGC
28	Insert-P6a-F	36	GGCCGGCCGGCCGGTTCTACATAAATGCCTAACGAC
29	Insert-P6a-R	41	ATATGCATGGCCGGCCGGCCAGTCCTACAATTTAGCACGGG
30	flexiTEV-f2	78	AACCTGTATTTTCAGGGCGGTGGCAGCGGCGGAGGGAGTGGTGGACAAGGAGATATACATATGGCTAGCATGAATCAC
31	flexiTEV-r	77	CTGAAAATACAGGTTTTCCCCGCCACTACCGCCACCGCTTCCTCCTTTATACAGTTCATCCATACCGTGGGTAATGC

32	IRES_Domain3_F	49	CCATGAAAACCTGTATTTTCAGGGCatTGCTCGCTCAAACATTAAGTGG
33	IRES_R2	39	CATGGTAAATTCTTTTTCTTGAAGTGAGATTCTTTTCGC
34	IRES_TEVDB_BB_F	50	ACTTCAAGAAAAAGAATTTACCATGGGTGAAGAACTGTTTACCGGCGTTG
35	IRES_TEVDB_BB_R	25	GCCCTGAAAATACAGGTTTTCATGG
36	IRES_23AA_F	52	GGGCTAACAGGAGGAATTAACCATGGGCatTGCTCGCTCAAACATTAAGTGG
37	PositiveCtrl_BB_R	32	CATGGTTAATTCCTCCTGTTAGCCCAAAAAAC
38	RtcB_F	44	AAGGAGATACATATGAATTACGAATTACTGACCACTGAAAATGC
39	RtcB_R	46	GGAGTGGTGAATCCGTTAGCGATTATCCTTTTACGCACACCACCTG
40	pBAD_BB_RtcB_F	22	TCGCTAACGGATTCACCACTCC
41	pBAD_BB_RtcB_R	40	TTCGTAATTCATATGTATCTCCTTCAGGTCGAGGTGGCCC
42	SD_lib_BB_F	20	GGTGAAGAACTGTTTACCGG
43	SD_lib_BB_R	21	GCCCTGAAAATACAGGTTTTC
44	SD_lib_insert_F	21	GAAAACCTGTATTTTCAGGGC
45	SD_lib_insert_R	20	CCGGTAAACAGTTCTTCACC
46	pBAD-BB_2_F	21	GTCTCCCCATGCGAGAGTAGG
47	pBAD-BB_2_R	24	ATGGAGAAACAGTAGAGAGTTGCG
48	TEVP_Fragment_F	31	AATGGAACACTGGTGGTCCAATCACTACATG
49	TEVP_Fragment_R	35	ATATGCCATCACCTGAAGGGAATGTGCAACTAGTG
50	TEVP_BB_F	33	CATTCCCTTCAGGTGATGGCATATTCTGGAAGC
51	TEVP_BB_R	36	GACCACCAGTGTTCCATTATTTCTTCTAAACAAGTG
52	TEVP_BB_F2	25	TAAGGATCCTCTAGAGTCGACCTGC
53	TEVP_BB_R2	30	AAACAAGCTTTCTCCATGATGATGATGATG
54	Amp_silk_repetitive_unit_F	17	GGCGGTAGTGGCGGTTC
55	Gib_silk_tandem_seq_R	25	ATGGTGATGATGATGGTGACTAGTC
56	TEVDB_Permuted_F	57	AAAAAACCTAGGCACCATCATCATCACCACACCGGTTAATTGAGGCCTGAGTATAAG
57	TEVDB_Permuted_R	74	AAAAAACTAGTTTTGTGATTCATGCTAGCCATATGTATATCTCCTTGCGGTAGCATTATGTTCAGATAAGGTCG
58	Linearize_F	45	AAAAAACCTAGGCATCATCATCATCATCATTGAGTTTAAACGGTC
59	Linearize_R	37	AAAAAAACTAGTCATGGTTAATTCCTCCTGTTAGCCC
60	pBAD_BB_RtcB_F	22	TCGCTAACGGATTCACCACTCC
61	pBAD_BB_RtcB_R	40	TTCGTAATTCATATGTATCTCCTTCAGGTCGAGGTGGCCC
62	RtcB_F	52	GCCGGGCCACCTCGACCTGAATGAATTACGAATTACTGACCACTGAAAATGC
63	RtcB_R	44	GAGGTGCCGCCGGCTTCCATTTATCCTTTTACGCACACCACCTG
64	Biotinylated GFP Probe	26	/5BiosG/GGTCAGGGTGGTCACCAGGGTCGGCC
65	PosCTRL_BB_F	21	TAAAGCTCGAGCGAAGCTTGG
66	tRBSdX_BB_R	43	CCCTGAAAATACAGGTTTTCATGGTGATGATGATGGTGGCTGC
67	mCherry-tRBSdX-F	40	GAAAACCTGTATTTTCAGGGCATGGTGAGCAAGGGCGAGG
68	mCherry-posCTRL_R	40	AAGCTTCGCTCGAGCTTTACTTGTACAGCTCGTCCATGCC

69	TEV-DB-BB-F	55	GGCAGCAGCGAGAATCTTTATTTCCAAGGTGGTGAAGAACTGTTTACCGGCGTTG
70	TEV-DB-BB-R	33	TTTGTGATTCATGCTAGCCATATGTATATCTCC
71	mCherry-TEV-DB-F	39	TGGCTAGCATGAATCACAAAATGGTGAGCAAGGGCGAGG
72	mCherry-R	51	ATAAAGATTCTCGCTGCTGCCGCTGCTGCCCTTGTACAGCTCGTCCATGCC
GeneBlocks (Letters in red indicate homology arms)			
	Name	**Length (bp)**	**Sequences (5' to 3')**
1	td-FP-G-td	1199	TCGCAACTCTCTACTGTTTCTCCATACCCGTTTTTTGGGCTACGCTGAATTCGAATTGGTTCTACATAAATGCCTAACGACTATCCCTTTGGGGAGTAGGGTCAAGTGACTCGAAACGATAGACAACTTGCTTTAACAAGTTGGAGATATAGTCTGCTCTGCATGGTGACATGCAGCTGGATATAATTCCGGGGTAAGATTAACGACCTTATCTGAACATAATGCTACCGTTTAATATTAAACTGCCGGTTCCGTGGCCGACCCTGGTGACCACCCTGACCTATGGCGTTCAGTGCTTTAGCCGCTATCCGGATCATATGAAACGCCATGATTTCTTTAAAAGCGCGATGCCGGAAGGCTATGTGCAGGAACGTACCATTAGCTTCAAAGATGATGGCACCTATAAAACCCGTGCGGAAGTTAAATTTGAAGGCGATACCCTGGTGAACCGCATTGAACTGAAAGGTATTGATTTTAAAGAAGATGGCAACATTCTGGGTCATAAACTGGAATATAATTTCAACAGCCATAACGTGTATATTACCGCCGATAAACAGAAAAATGGCATCAAAGCGAACTTTAAAATCCGTCACAACGTGGAAGATGGTAGCGTGCAGCTGGCGGATCATTATCAGCAGAATACCCCGATTGGTGATGGCCCGGTGCTGCTGCCGGATAATCATTATCTGAGCACCCAGAGCGTTCTGAGCAAAGATCCGAATGAAAAACGTGATCATATGGTGCTGCTGGAATTTGTTACCGCCGCGGGCATTACCCACGGTATGGATGAACTGTATAAAGGCAGCCACCATCATCATCACCATTAATTAAACGGTCTCCAGCTTGGCTGTTTTGGCGGATAACAGGAGGAATTAACCATGGTTAGCAAAGGTGAAGAACTGTTTACCGGCGTTGTGCCGATTCTGGTGGAACTGGATGGTGATGTGAATGGCCATAAATTTAGCGTTCGTGGCGAAGGCGAAGGTGATGCGACCAACGGTAAACTGACCCTGAAATTTATTTGCACCACCGGTGATGTTTTCTTGGGTTAATTGAGGCCTGAGTATAAGGTGACTTATACTTGTAATCTATCTAAACGGGGAACCTCTCTAGTAGACAATCCCGTGCTAAATTGTAGGACTATGCATATCCTTAGCGAAAGCTAAGGATTTTTTTTGTCTCCCCATGCGAGAGTAGGG
2	Ribozyme	1038	TCGCAACTCTCTACTGTTTCTCCATACCCGTTTTTTGGGCTACGCTGAATTCCCGGCAGTTTCCCGGTCCCAAGCCCGGATAAAGCTCGAGGGGGCGGGAAACCGCCTAAGAGCGCGAAACTGCCGGTTCCGTGGCCGACCCTGGTGACCACCCTGACCTATGGCGTTCAGTGCTTTAGCCGCTATCCGGATCATATGAAACGCCATGATTTCTTTAAAAGCGCGATGCCGGAAGGCTATGTGCAGGAACGTACCATTAGCTTCAAAGATGATGGCACCTATAAAACCCGTGCGGAAGTTAAATTTGAAGGCGATACCCTGGTGAACCGCATTGAACTGAAAGGTATTGATTTTAAAGAAGATGGCAACATTCTGGGTCATAAACTGGAATATAATTTCAACAGCCATAACGTGTATATTACCGCCGATAAACAGAAAAATGGCATCAAAGCGAACTTTAAAATCCGTCACAACGTGGAAGATGGTAGCGTGCAGCTGGCGGATCATTATCAGCAGAATACCCCGATTGGTGATGGCCCGGTGCTGCTGCCGGA

			TAATCATTATCTGAGCACCCAGAGCGTTCTGAGCAAAGATCCGAAT GAAAAACGTGATCATATGGTGCTGCTGGAATTTGTTACCGCCGCGG GCATTACCCACGGTATGGATGAACTGTATAAAGGCAGCCACCATCA TCATCACCATGAAAACCTGTATTTTCAGGGCCAAGGAGATATACAT ATGGCTAGCATGAATCACAAAATGGTTAGCAAAGGTGAAGAACTG TTTACCGGCGTTGTGCCGATTCTGGTGGAACTGGATGGTGATGTGA ATGGCCATAAATTTAGCGTTCGTGGCGAAGGCGAAGGTGATGCGA CCAACGGTAAACTGACCCTGAAATTTATTTGCACCACCGGTGTTTCG CGCAGTAACACTGCCAATGCCGGTCCCAAGCCCGGATAAAAGTGG AGGGCTGCGCGAAACATGCATATCCTTAGCGAAAGCTAAGGATTTT TTTTGTCTCCCCATGCGAGAGTAGGG
3	TEV2_Delta	686	CATCATGGAGAAAGCTTGTTTAAGGGACCACGTGATTACAACCCGA TATCGAGCACCATTTGTCATTTGACGAATGAATCTGATGGGCACAC AGCATCGTTGTATGGTATTGGATTTGGTCCCTTCATCATTACAAACA AGCACTTGTTTAGAAGAAATAATGGAACACTGTTGGTCCAATCACT ACATGGTGTATTCAAGGTCAAGAACACCACGACTTTGCAACAACAC CTCATTGATGGGAGGGACATGATAATTATTCGCATGCCTAAGGATT TCCCACCATTTCCTCAAAAGCTGAAATTTAGAGAGCCACAAAGGGA AGAGCGCATATGTCTTGTGACAACCAACTTCCAAACTAAGAGCATG TCTAGCATGGTGTCAGACACTAGTTGCACATTCCCTTCATCTGATGG CATATTCTGGAAGCATTGGATTCAAACCAAGGATGGGCAGTGTGGC AATCCATTAGTATCAACTAGAGATGGGTTCATTGTTGGTATACACTC AGCATCGAATTTCACCAACACAAACAATTATTTCACAAGCGTGCCG AAAAACTTCATGGAATTGTTGACAAATCAGGAGGCGCAGCAGTGG GTTAGTGGTTGGCGATTAAATGCTGACTCAGTATTGTGGGGGGGC CATAAAGTTTTCATGGTGTAATAAGGATCCTCTAGAGTCGA
Minigene (Colored in Blue: dragline silk sequence unit)			
	Name	**Length (bp)**	**Sequence (5’ to 3’)**
1	pIDT-silk unit	2058	CCCGTGTAAAACGACGGCCAGTTTATCTAGTCAGCTTGATTCTAGCT GATCGTGGACCGGAAGGTGAGCCAGTGAGTTGATTGCAGTCCAGT TACGCTGGAGTCTGAGGCTCGTCCTGAATGATATGCGGCCTCGGCG GTAGTGGCGGTTCTGCTAGCGGTAGAGGCGGGCTGGGTGGCCAGG GTGCAGGTGCGGCTGCGGCTGCCGCGGCAGCGGCCGCAGGCGGT GCCGGCCAAGGTGGCTATGGCGGCCTGGGTTCTCAGGGGACTAGT CACCATCATCATCACCATGCGCGTGATCTTACGGCATTATACGTATG ATCGGTCCACGATCAGCTAGATTATCTAGTCAGCTTGATGTCATAGC TGTTTCCTGAGGCTCAATACTGACCATTTAAATCATACCTGACCTCC ATAGCAGAAAGTCAAAAGCCTCCGACCGGAGGCTTTTGACTTGATC GGCACGTAAGAGGTTCCAACTTTCACCATAATGAAATAAGATCACT ACCGGGCGTATTTTTTGAGTTATCGAGATTTTCAGGAGCTAAGGAA GCTAAAATGAGCCATATTCAACGGGAAACGTCTTGCTTGAAGCCGC GATTAAATTCCAACATGGATGCTGATTTATATGGGTATAAATGGGC TCGCGATAATGTCGGGCAATCAGGTGCGACAATCTATCGATTGTAT GGGAAGCCCGATGCGCCAGAGTTGTTTCTGAAACATGGCAAAGGT AGCGTTGCCAATGATGTTACAGATGAGATGGTCAGGCTAAACTGGC TGACGGAATTTATGCCTCTTCCGACCATCAAGCATTTTATCCGTACTC CTGATGATGCATGGTTACTCACCACTGCGATCCCAGGGAAAACAGC

			ATTCCAGGTATTAGAAGAATATCCTGATTCAGGTGAAAATATTGTTG ATGCGCTGGCAGTGTTCCTGCGCCGGTTGCATTCGATTCCTGTTTGT AATTGTCCTTTTAACGGCGATCGCGTATTTCGTCTCGCTCAGGCGCA ATCACGAATGAATAACGGTTTGGTTGGTGCGAGTGATTTTGATGAC GAGCGTAATGGCTGGCCTGTTGAACAAGTCTGGAAAGAAATGCAT AAACTCTTGCCATTCTCACCGGATTCAGTCGTCACTCATGGTGATTT CTCACTTGATAACCTTATTTTTGACGAGGGGAAATTAATAGGTTGTA TTGATGTTGGACGAGTCGGAATCGCAGACCGATACCAGGATCTTGC CATCCTATGGAACTGCCTCGGTGAGTTTTCTCCTTCATTACAGAAAC GGCTTTTTCAAAAATATGGTATTGATAATCCTGATATGAATAAATTG CAGTTTCACTTGATGCTCGATGAGTTTTTCTAATGAGGACCTAAATG TAATCACCTGGCTCACCTTCGGGTGGGCCTTTCTGCGTTGCTGGCGT TTTTCCATAGGCTCCGCCCCCCTGACGAGCATCACAAAAATCGATGC TCAAGTCAGAGGTGGCGAAACCCGACAGGACTATAAAGATACCAG GCGTTTCCCCCTGGAAGCTCCCTCGTGCGCTCTCCTGTTCCGACCCT GCCGCTTACCGGATACCTGTCCGCCTTTCTCCCTTCGGGAAGCGTGG CGCTTTCTCATAGCTCACGCTGTAGGTATCTCAGTTCGGTGTAGGTC GTTCGCTCCAAGCTGGGCTGTGTGCACGAACCCCCCGTTCAGCCCG ACCGCTGCGCCTTATCCGGTAACTATCGTCTTGAGTCCAACCCGGTA AGACACGACTTATCGCCACTGGCAGCAGCCACTGGTAACAGGATTA GCAGAGCGAGGTATGTAGGCGGTGCTACAGAGTTCTTGAAGTGGT GGCCTAACTACGGCTACACTAGAAGAACAGTATTTGGTATCTGCGC TCTGCTGAAGCCAGTTACCTCGGAAAAAGAGTTGGTAGCTCTTGAT CCGGCAAACAAACCACCGCTGGTAGCGGTGGTTTTTTTGTTTGCAA GCAGCAGATTACGCGCAGAAAAAAAGGATCTCAAGAAGATCCTTTG ATTTTCTACCGAAGAAAGGCCCA

Table S2. Buffer Compositions. Composition of the buffers that were used in Western blot for silk constructs.

10X Buffer A	
	Final Concentration (mM)
Trsi Base	10
5M HCl	5
NaH_2PO_4	200

Lysis Buffer (5 mL)		
	Amount	Final Concentration (M)
Urea	2.4 g	8
Thiourea	0.75 g	2
10X buffer A	500 uL	1X

V. Supplementary References

(1) Shub, D. A.; Gott, J. M.; Xu, M. Q.; Lang, B. F.; Michel, F.; Tomaschewski, J.; Pedersen-Lane, J.; Belfort, M. Structural Conservation among Three Homologous Introns of Bacteriophage T4 and the Group I Introns of Eukaryotes. *Proc. Natl. Acad. Sci. U. S. A.* **1988**, *85* (4), 1151–1155. https://doi.org/10.1073/pnas.85.4.1151.

(2) Perriman, R.; Ares, M. Circular MRNA Can Direct Translation of Extremely Long Repeating- Sequence Proteins in Vivo. *Rna* **1998**, *4* (9), 1047–1054. https://doi.org/10.1017/S135583829898061X.

(3) Perriman, R. Circular MRNA Encoding for Monomeric and Polymeric Green Fluorescent Protein. *Methods Mol. Biol.* **2001**, *183*, 69–85. https://doi.org/10.1385/1-59259-280-5:069.

(4) Ford, E.; Ares Jr., M. Synthesis of Circular RNA in Bacteria and Yeast Using RNA Cyclase Ribozymes Derived from a Group I Intron of Phage T4. *Proc. Natl. Acad. Sci. USA* **1994**, *91* (8), 3117–3121.

(5) Fang, J.; Chen, L.; Cheng, B.; Fan, J. Engineering Soluble Tobacco Etch Virus Protease Accompanies the Loss of Stability. *Protein Expr. Purif.* **2013**, *92* (1), 29–35. https://doi.org/10.1016/j.pep.2013.08.015.

(6) Sanchez, M. I.; Ting, A. Y. Directed Evolution Improves the Catalytic Efficiency of TEV Protease. *Nat. Methods* **2020**, *17* (2), 167–174. https://doi.org/10.1038/s41592-019-0665-7.

(7) Colussi, T. M.; Costantino, D. A.; Zhu, J.; Donohue, J. P.; Korostelev, A. A.; Jaafar, Z. A.; Plank, T. D. M.; Noller, H. F.; Kieft, J. S. Initiation of Translation in Bacteria by a Structured Eukaryotic IRES RNA. *Nature* **2015**, *519* (7541), 110–113. https://doi.org/10.1038/nature14219.

(8) Litke, J. L.; Jaffrey, S. R. Highly Efficient Expression of Circular RNA Aptamers in Cells Using Autocatalytic Transcripts. *Nat. Biotechnol.* **2019**, *37* (6), 667–675. https://doi.org/10.1038/s41587-019-0090-6.

(9) Filipowicz, W.; Shatkin, A. J. Origin of Splice Junction Phosphate in TRNAs Processed by HeLa Cell Extract. **1983**, *32* (February), 547–557.

(10) Laski, F. A.; Fire, A. Z.; Rajbhandarys, U. L.; Sharp, P. A. Characterization of TRNA Precursor Splicing in Mammalian Extracts*. **1983**, *258* (19), 11974–11980. https://doi.org/10.1016/S0021-9258(17)44327-4.

(11) Englert, M.; Xia, S.; Okada, C.; Nakamura, A.; Tanavde, V.; Yao, M.; Eom, S. H.; Konigsberg, W. H.; Wang, J. Structural and Mechanistic Insights into Guanylylation of RNA-Splicing Ligase RtcB Joining RNA Between. **2012**. https://doi.org/10.1073/pnas.1213795109.

(12) Popow, J.; Englert, M.; Weitzer, S.; Schleiffer, A.; Mierzwa, B.; Mechtler, K.; Trowitzsch, S.; Will, C. L.; Lührmann, R.; Söll, D.; Martinez, J. HSPC117 Is the Essential Subunit of a Human TRNA Splicing Ligase Complex. *Science* **2011**, *331* (6018), 760–764. https://doi.org/10.1126/science.1197847.

(13) Tanaka, N.; Chakravarty, A. K.; Maughan, B.; Shuman, S. Novel Mechanism of RNA Repair by RtcB via Sequential 2', 3'- Cyclic Phosphodiesterase and 3'-

Phosphate/5'-Hydroxyl Ligation Reactions. *J. Biol. Chem.* **2011**, *286* (50), 43134–43143. https://doi.org/10.1074/jbc.M111.302133.
(14) Tanaka, N.; Meineke, B.; Shuman, S. RtcB , a Novel RNA Ligase , Can Catalyze TRNA Splicing and HAC1 MRNA Splicing in Vivo. *J. Biol. Chem.* **2011**, *286* (35), 30253–30257. https://doi.org/10.1074/jbc.C111.274597.
(15) Tanaka, N.; Shuman, S. RtcB Is the RNA Ligase Component of an Escherichia Coli RNA Repair Operon. *J. Biol. Chem.* **2011**, *286* (10), 7727–7731. https://doi.org/10.1074/jbc.C111.219022.
(16) Das, U.; Shuman, S. 2′-Phosphate Cyclase Activity of RtcA : A Potential Rationale for the Operon Organization of RtcA with an RNA Repair Ligase RtcB in Escherichia Coli and Other Bacterial Taxa. **2013**, 1355–1362. https://doi.org/10.1261/rna.039917.113.1.
(17) Van Den Berg, S.; Löfdahl, P. Å.; Härd, T.; Berglund, H. Improved Solubility of TEV Protease by Directed Evolution. *J. Biotechnol.* **2006**, *121* (3), 291–298. https://doi.org/10.1016/j.jbiotec.2005.08.006.
(18) Kapust, R. B.; Tözsér, J.; Fox, J. D.; Anderson, D. E.; Cherry, S.; Copeland, T. D.; Waugh, D. S. Tobacco Etch Virus Protease: Mechanism of Autolysis and Rational Design of Stable Mutants with Wild-Type Catalytic Proficiency. *Protein Eng.* **2001**, *14* (12), 993–1000. https://doi.org/10.1093/protein/14.12.993.